

Effects of needle peening and shot peening for stainless steel welded joint on the crack size rendered harmless

Ryutaro Fueki ^a, Koji Takahashi ^a, Mitsuru Handa ^b

^aYokohama National University, Japan, fueki-ryuutaro-pv@ynu.jp takahashi-koji-ph@ynu.ac.jp

^bToyo Seiko co., Ltd., Japan, m_handa@toyoseiko.co.jp

Keywords: Needle peening; shot peening; fatigue limit; welded joint; compressive residual stress

Introduction

Welded joints are often used in large steel structures. Fatigue cracks tend to initiate at the welded joints (especially at the weld toe) due to tensile residual stresses and stress concentration. Tensile residual stresses result from the effects of heat applied during the welding process. A discontinuous portion of the weld beads cause stress concentration.

Peening methods such as needle peening (NP) and shot peening (SP) are expected to be effective for improving fatigue strength of welded joints. Non-destructive inspections are typically conducted prior to performing peening on welded joints in steel structures. However, detection limits are associated with non-destructive inspection, and it is not possible to detect cracks below a certain size. The reliability of welded joints is decreased by the undetected cracks. It is possible to improve reliability of welded joints if peening can be used to mitigate the effect of the fatigue cracks.

Recently, Houjou *et al.* [1] reported that the fatigue limit of a stainless steel welded joint containing a crack-like surface defect at the weld toe could be improved by NP and surface defects could be rendered harmless by NP. However, the effects of SP on the fatigue limit of welded joints with surface defects are unclear.

Objectives

The objective of the present study involved evaluating the effects of NP and SP on the fatigue limit of butt-welded joints of austenitic stainless steel containing a crack-like defects on a weld toe and discuss the difference between NP and SP.

Methodology

SP was applied to butt-welded specimens with a semi-circular slit on a weld toe, and bending fatigue tests were carried out. The fatigue test results were compared with those for NP-treated specimens obtained in prior studies [1]. This is followed by describing several factors that affect fatigue strength. Residual stress distribution of the weld toe was measured using X-ray diffraction (XRD).

Test method

The test material corresponded to austenitic stainless steel (JIS-SUS316). Its chemical composition and mechanical properties are shown in Tables 1 and 2, respectively. The test specimen was cut out from the butt-welded plate. The shape and dimension of the specimen are shown in Fig. 1 (a). A semi-circular slit similar to a surface crack was introduced within 0.2 mm of the weld toe as shown in Fig. 1(b). SP was performed around the weld bead as shown in Fig. 2. The SP conditions are shown in Table 3. The details of NP-treated specimens and NP conditions can be found in the previous study [1]. Plane bending fatigue tests

Table1 Chemical composition of SUS316

[Unit: mass%]

C	Si	Mn	P	S	Ni	Cr	Mo
0.05	0.71	1.04	0.033	0.002	10.07	16.81	2.09

Table 2 Mechanical properties of SUS316

0.2% proof Stress [MPa]	Ultimate tensile strength [MPa]	Elongation [%]	Hardness
307	628	55	180HV

were performed with constant load amplitudes at a stress ratio of $R = 0$. All the tests were performed at a frequency of $f = 20$ Hz. The fatigue limit was defined as the maximum stress amplitude at which the specimen can endure 5×10^6 cycles.

Measurement of residual stress

The longitudinal residual stress of the weld toe before and after peening was measured by using XRD with Cr-K α radiation. In-depth residual stress distributions were obtained by alternately measuring the residual stress on the surface and applying chemical etching to remove the surface layer.

Measurement of hardness

The Vickers hardness at the cross section of the weld toe was measured with an indentation load of 4.9 N with a hold time of 20 s.

Results and analysis

Fatigue test results

Figures 3 and 4 summarize the relationship between the stress amplitude (σ_a) and the depth of the semi-circular slit (a) based on fatigue test results. Figure 3 shows the test results for SP and Non-SP specimens, while Fig. 4 shows those for NP and Non-NP specimens [1]. Solid symbols denote the specimens that endured 5×10^6 cycles without exhibiting fracture. The asterisks (*) in Fig. 4 indicate the specimens that fractured at locations other than the semi-circular slit. The difference of fatigue strength between Non-SP and Non-NP specimen resulted from cutting the specimens from different welded plates. The fatigue limits of all specimens increased by 80–83% due to SP and 60–133% due to NP. Figures 3 and 4 show that SP had a higher ability than NP for improving the fatigue limit of the welded specimen without a slit.

Definition of rendering a semi-circular slit harmless

A slit is considered harmless if the fatigue test results satisfy either of the following two conditions [1]:

Condition (a): The fatigue limit of the peened specimen containing a semi-circular slit increased to more than 95% of that without a semi-circular slit.

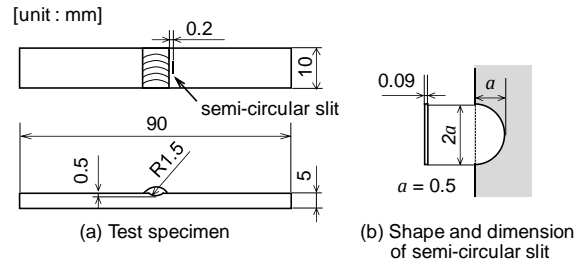


Fig. 1 Shape and dimensions of test specimen

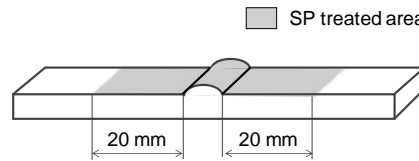


Fig. 2 SP treating location

Table 3 SP conditions

Peening machine	Direct pressure peening
Air pressure	0.2 MPa
Shot	Conditioned cut wire shot
Shot diameter	ϕ 0.67 mm
Shot hardness	600HV
Shot time	17 s
Shot distance	90 mm
Coverage	300%
Arc height	0.26 mm (A)

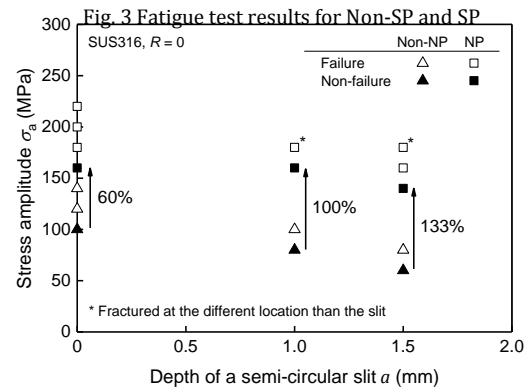
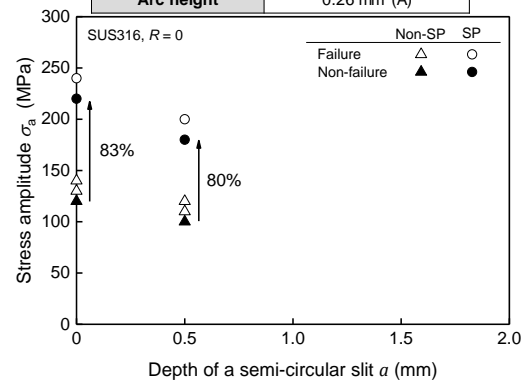


Fig. 4 Fatigue test results for Non-NP and NP [1]

Condition (b): The peened specimen with a semi-circular slit fractured at a location other than the slit. Figure 3 shows that the fatigue test results for SP specimen with a slit depth of 0.5 mm satisfied neither of above two conditions. This result indicates that the acceptable slit size a_{max} after SP was smaller than 0.5 mm. From Fig. 4, the fatigue limit of a NP specimen with a slit depth of 1.0 mm is equivalent to that of a NP specimen without a slit. This situation satisfies condition (a). However, the fatigue test results for NP specimen with a slit depth of 1.5 mm satisfied neither of above two conditions. Therefore, a_{max} after NP was more than 1.0 mm and smaller than 1.5 mm.

Residual stress distributions

Figure 5 shows the longitudinal residual stress distributions for SP and Non-SP specimens, while Fig. 6 shows those for NP and Non-NP specimens. From Fig. 5 and 6, the tensile residual stress induced at the surface of the weld toe due to the effects of heat applied during the welding process changed to a compressive residual stress after SP and NP. The surface compressive residual stress after SP approximately corresponded to 500 MPa. The maximum compressive residual stress after SP corresponded to 570 MPa, measured at a depth of 0.05 mm. The surface compressive residual stress after NP was approximately 350 MPa. The maximum compressive residual stress after NP was 500 MPa, measured at a depth of 0.05 mm. The results indicate that the surface and the maximum compressive residual stress after SP were larger than those after NP. The distance from the surface to the zero residual stress point (crossing point) for SP and NP specimen was approximately 0.4 mm and 1.4 mm, respectively. The crossing point for SP specimen was much smaller than that for NP specimen.

Hardness at the weld toe

The residual stress after SP and NP near the surface layer exceeded the yield stress before peening treatment, as shown in Fig. 5 and 6. It appeared to be caused by an increase in yield stress due to hardening. The Vickers hardness was measured to verify the hypothesis.

Figures 7 and 8 shows the in-depth hardness profiles measured at the weld toe. From Fig. 7, the hardness at the surface after SP and NP corresponded to 360 HV and 400 HV, respectively, which were more than twice

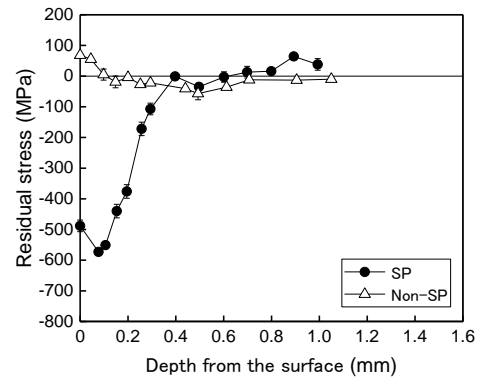


Fig. 5 Residual stress distribution before and after SP

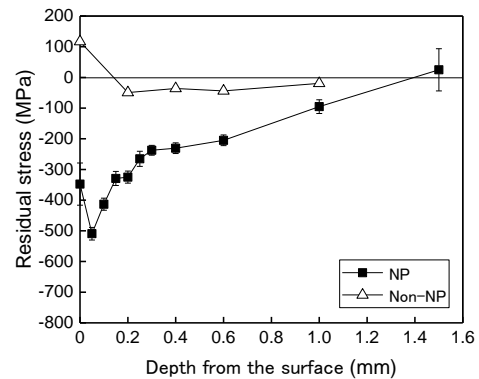


Fig. 6 Residual stress distribution before and after NP

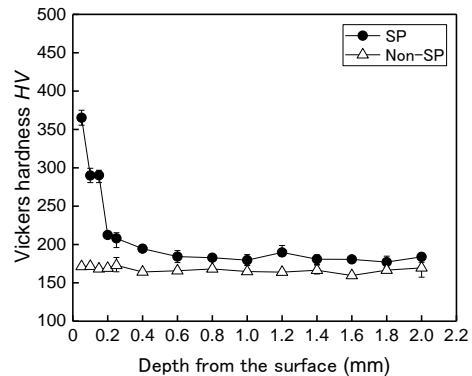


Fig. 7 Measurement results for Non-SP and SP

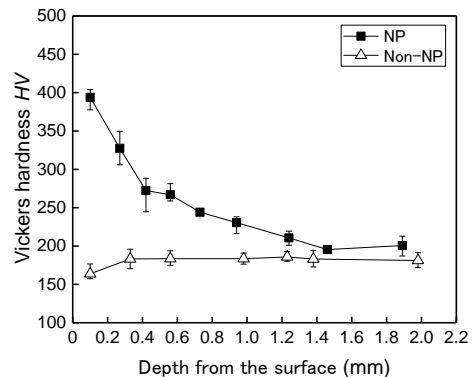


Fig. 8 Measurement results for Non-NP and NP

that of the non-peened sample. The hardness of SP specimens decreased until it reached a value of 180 HV at a depth of 0.6 mm. The hardness of NP specimens gradually decreased until it reached a value of 180 HV as shown in Fig. 8. The depth was 1.4 mm, which was much deeper than that of SP specimens.

Analysis of stress concentration of the weld toe

Finite element method analysis was conducted to clarify the changes in the stress concentration of the weld toe due to SP and NP. The models correspond to symmetric half models of the welded specimen that consist of a 20-node hexahedral element with a minimum element size of 0.03 mm. The results of the elastic analysis using universal analysis software (ANSYS 14.5) are shown in Fig. 9 and 10 as a contour of the X-direction stress σ_x around the weld zone at a nominal stress σ_{nom} of 200 MPa. Additionally, σ_{nom} denote the nominal stress for a non-welded specimen at the same position as that of the weld toe. Figures 11 and 12 shows the X-direction stress distribution at the weld toe obtained from Fig. 9 and 10. The stress concentration factor α can be calculated by comparing the stress with the nominal stress. The α of the weld toe after SP decreased from 2.3 to 2.0 due to the shape improvement caused by SP, while that after NP decreased from 2.5 to 1.7. The results indicate that the stress concentration of the weld toe was more relaxed by NP than SP.

Estimation of the acceptable semi-circular slit size

The acceptable semi-circular slit size a_{max} was estimated by comparing the magnitude of the relationship between the positive value of the stress intensity factor range ΔK_T and the threshold stress intensity factor range ΔK_{th} . ΔK_T can be calculated as follows:

$$\Delta K_T = K_{max} + K_r \quad (1)$$

where K_{max} denotes the maximum stress intensity factor due to applied stress, and K_r denotes the stress intensity factor due to residual stress. In the study, the values of K_{max} and K_r were evaluated using FEM analysis for a quarter specimen model with a semi-circular crack. As widely-known, the threshold stress intensity factor range ΔK_{th} depends on the crack size [2]. An equation relating ΔK_{th} and the crack length was proposed by Tange *et al.* [3] as follows:

$$\Delta K_{th} = \left\{ \left(\frac{1}{\Delta K(L)_{th}} \right)^2 + \left(\frac{1}{\alpha \Delta \sigma_{w0} \sqrt{\pi a}} \right)^2 \right\}^{-1/2} \quad (2)$$

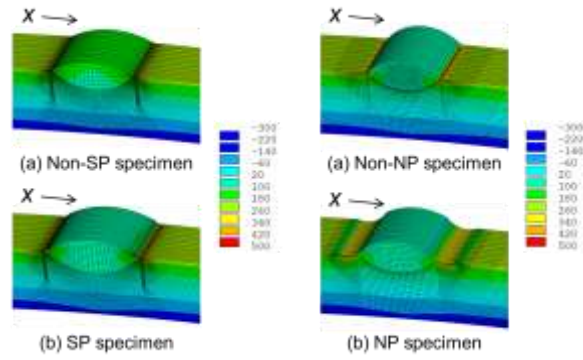


Fig. 9 Contour of the X-direction stress before and after SP

Fig. 10 Contour of the X-direction stress before and after NP

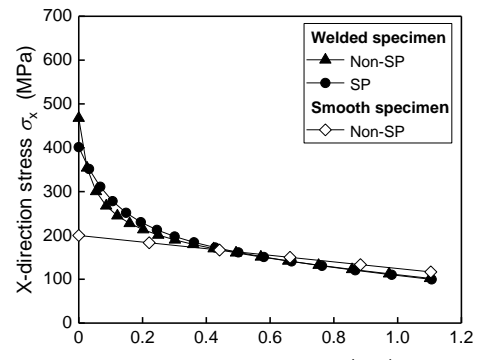


Fig.11 Applied stress distribution for Non-SP and SP

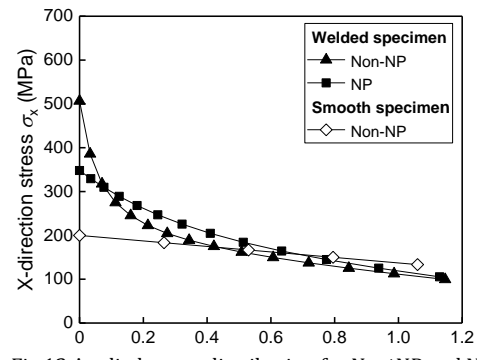


Fig.12 Applied stress distribution for NP and NP

where $\Delta K(L)_{th}$ denotes the threshold stress intensity factor range for a large crack, and $\Delta\sigma_{w0}$ denotes the stress range at the fatigue limit for non-peened specimens without defects. In the study, $\Delta K(L)_{th}$ corresponded to $6.5 \text{ MPa}\cdot\text{m}^{1/2}$ [4], and $\Delta\sigma_{w0}$ corresponded to 380 MPa as calculated from the experimental results presented by Nakajima *et al.* [5]. Additionally, a denotes the depth of a semi-circular crack, and α is the shape parameter that is obtained via the Newman–Raju Equation [6].

The semi-circular crack can be considered as a non-propagating crack if ΔK_T is lower than the threshold stress intensity factor range ΔK_{th} . Therefore, when ΔK_T is equal to ΔK_{th} , the depth of the crack is equivalent to the upper limit depth of the non-propagating crack a_{lim} for a given stress amplitude. Therefore, when the stress amplitude is equal to the fatigue limit of a peened specimen without a semi-circular slit, then a_{lim} is equivalent to the maximum depth of the semi-circular slit a_{max} that can be rendered harmless. As shown in Fig. 13 and 14, the intersection between ΔK_T and ΔK_{th} corresponds to the maximum semi-circular slit size a_{max} .

The value of a_{max} after SP was 0.11 mm . This result was consistent with the experimental results: The value of a_{max} after SP was smaller than 0.5 mm .

The value of a_{max} after NP was 1.10 mm , which was much larger than that after SP. This result was consistent with the experimental results: The value of a_{max} after NP was more than 1.0 mm and smaller than 1.5 mm .

Prediction of fatigue limit with a semi-circular slit

The value of fatigue limit σ_w with a semi-circular slit was obtained by determining a_{lim} for several levels of stress amplitude σ_a in the same manner as that described in prior section. The prediction lines of σ_w for each depth of slit are shown in Fig. 15 and 16. The fatigue test results shown in Fig. 3 and 4 are also shown in Fig. 15 and 16. The prediction results for the cases before and after SP as well as before and after NP matched well with the experimental results.

Conclusions

The present study involved evaluating the effects of needle peening (NP) and shot peening (SP) on the fatigue limit of butt-welded joints of austenitic stainless steel containing crack-like defects on a weld toe and discuss the difference between NP and SP. The following results were obtained:

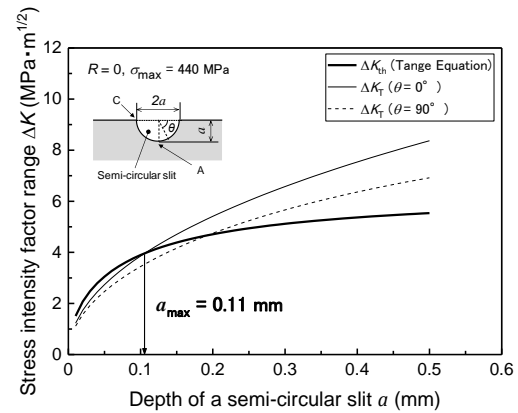


Fig. 13 Estimation results of acceptable slit size after SP

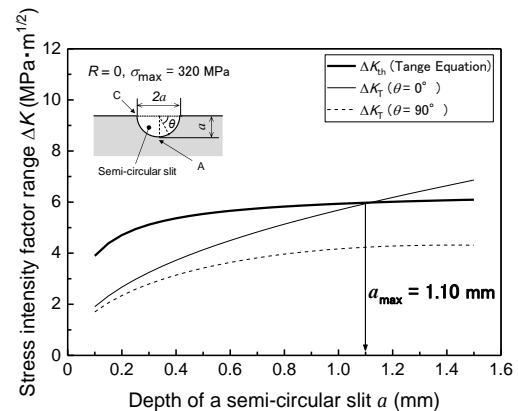


Fig. 14 Estimation results of acceptable slit size after NP

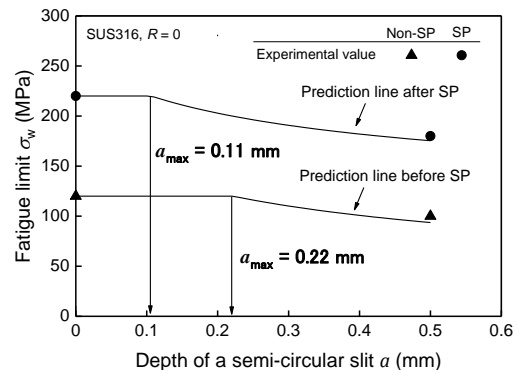


Fig. 15 Fatigue limit prediction before and after SP

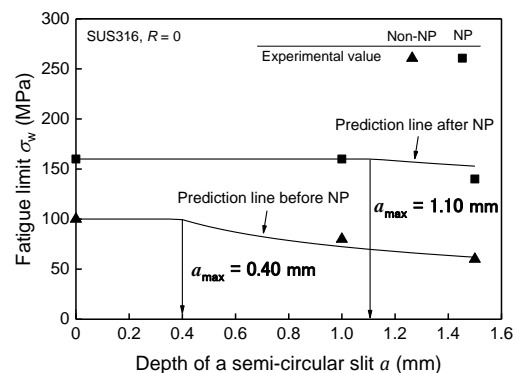


Fig. 16 Fatigue limit prediction before and after NP

- (1) The fatigue limits of all specimens increased by 80–83% due to SP and 60–133% due to NP. SP had a higher ability than NP for improving the fatigue limit of the welded specimen without a slit.
- (2) Fatigue test results indicate that the acceptable slit size a_{\max} after SP was smaller than 0.5 mm and a_{\max} after NP was more than 1.0 mm and smaller than 1.5 mm.
- (3) The surface and the maximum compressive residual stress after SP were larger than those after NP. The distance from the surface to the zero residual stress point (crossing point) for SP specimen was much smaller than that for NP specimen.
- (4) The hardness at the surface after SP and NP corresponded to 360 HV and 400 HV, respectively, which were more than twice that of the non-peened sample. The hardness of SP specimens decreased until it reached a value of 180 HV at a depth of 0.6 mm. The hardness of NP specimens gradually decreased until it reached a value of 180 HV. The depth was 1.4 mm, which was much deeper than that of SP specimens.
- (5) The stress concentration factor of the weld toe after SP decreased from 2.3 to 2.0 due to the shape improvement caused by SP, while that after NP decreased from 2.5 to 1.7. The results indicate that the stress concentration of the weld toe was more relaxed by NP than SP.
- (6) The values of a_{\max} after SP and NP were 0.11 mm and 1.10 mm, respectively. This result was consistent with the experimental results. The estimation results indicate that a_{\max} after SP was much larger than that after NP.
- (7) The fatigue limit prediction results for the cases before and after SP as well as before and after NP matched well with the experimental results.

Considering the results above, it can be concluded SP had a higher ability than NP for improving the fatigue limit of the welded specimen without a slit. However, NP is more effective than SP for welded joint in terms of the defect size that can be rendered harmless.

Acknowledgements

A part of this work was supported by Grant-in-Aid for JSPS Fellows Grant Number 17J00191.

References

- [1] Houjou, K., Takahashi, K., Ando, K. and Abe, H. (2014), "Effect of peening on the fatigue limit of welded structural steel with surface crack, and rendering the crack harmless", *International Journal of Structural Integrity*, Vol. 5, pp. 279-289.
- [2] El Haddad, M.H., Topper, T.H. and Smith, K.N. (1979), "Prediction of non propagating cracks", *Engineering Fracture Mechanics*, Vol. 11, pp. 573-584.
- [3] Tange, A., Akutu, T. and Takamura, A., (1991), "Relation between shot-peening residual stress distribution and fatigue crack propagation life in spring steel", *Transactions of JSSE*, Vol. 36, pp. 47-53.
- [4] The Society of Materials Science, Japan, (1983), "Data book on fatigue crack growth rates of metallic materials", Vol. 2, Japan, pp. 458-459.
- [5] Nakajima, M., Akita, M., Uematsu, Y., and Tokaji, K. (2007), "Effects of prestrain on fatigue behavior in type 316 stainless steel", *Transactions of JSME Ser. A*, Vol. 73, pp. 796-802.
- [6] Newman, J.C., Jr. and Raju, I.S. (1981), "An empirical stress-intensity factor equation for the surface crack", *Engineering Fracture Mechanics*, Vol. 15, pp. 185-192.